N O T I C E

THIS DOCUMENT HAS BEEN REPRODUCED FROM
MICROFICHE. ALTHOUGH IT IS RECOGNIZED THAT
CERTAIN PORTIONS ARE ILLEGIBLE, IT IS BEING RELEASED
IN THE INTEREST OF MAKING AVAILABLE AS MUCH
INFORMATION AS POSSIBLE

Analysis for Predicting Adiabatic Wall Temperatures with Single Hole Coolant Injection into a Low Speed Crossflow

C. R. Wang, S. S. Papell, and R. W. Graham
Lewis Research Center
Cleveland, Ohio

NASA

ANALYSIS FOR PREDICTING ADIABATIC WALL TEMPERATURES WITH SINGLE

HOLE COOLANT INJECTION INTO A LOW SPEED CROSSFLOW

by C. R. Wang, S. S. Papell, and R. W. Graham

National Aeronautics and Space Administration
Lewis Research Center
Cleveland, Ohio 44135

NOMENCLATURE

A	coolant mixing layer cross sectional area
C	circumference of the cross sectional area
c_D	drag coefficient
c_p	constant pressure specific heat
D	major axis of ellipse
D_0	injection hole diameter
d	minor axis of ellipse
f_1, f_2, f_3	empirical constants in eq. (6)
e	normal distance from the wall to mixing layer centerline
h	height of coolant mixing layer (along the centerline)
M	Mach number
m	entrainment mass flow rate
p	static pressure
R	ideal gas constant
S	starting location of boundary layer flow
T	local total temperature
T_{oc}	injectant total temperature
$T_{o\infty}$	crossflow total temperature
T_{aw}	local adiabatic wall temperature
U	inviscid flow velocity within the coolant mixing layer
U_b	velocity within the boundary layer
U_j	coolant velocity
U_∞	crossflow velocity
X	distance along the wall surface ($X = 0$ at S)
Y	distance normal to the wall surface
Z, Z_0	coordinates along the coolant mixing layer centerline
α_0	inclination angle of the injection hole
δ	boundary layer thickness
η	film cooling effectiveness, $(T_{o\infty} - T_{aw})/(T_{o\infty} - T_{oc})$
θ	inviscid flow direction within the coolant mixing layer
λ	dimensionless injection mass flow rate, $\rho_j U_j / \rho_\infty U_\infty$
μ	viscosity
ρ	density of the coolant mixing layer
ρ_j	coolant density
ρ_∞	crossflow density
τ_w	wall shear stress

INTRODUCTION

Interest in surface cooling, boundary layer control and mixing process has promoted research in film cooling and blowing over a flat plate. For the film cooling application, normal injection, tangential slot injection, and injection through inclined holes have been the subjects of theoretical and experimental investigations to predict the film cooling effectiveness, $\eta = (T_{0\infty} - T_{aw})/(T_{0\infty} - T_{0c})$, and the surface heat transfer rate (refs. 1 to 5).

In most studies of film cooling with slot or discrete hole injection, the local adiabatic wall temperature was computed from the measured heat transfer rate. For this process, the boundary layer analysis was used. However, within the region near the injection, strong mixing invalidates the use of the heat transfer coefficient based on a well-developed boundary layer.

A systematic study of coolant injection through a hole into a crossflow and the concept of an equivalent slot width to correlate all data of slot and hole injection was described in reference 3. The experimental investigation of the effects of constant mainstream acceleration on effectiveness and heat transfer has shown that the mainstream acceleration increases the effectiveness downstream of a single hole (ref. 4). The interaction due to a jet entering normally into a freestream has been studied with particular attention to the visualization of the large scale flow interaction (ref. 5), and the film cooling downstream from a single normal jet yields a lower centerline effectiveness compared to an inclined jet because of greater mixing with freestream. In reference 6 infrared thermography was used to measure the local adiabatic wall temperatures in the film cooled area of a plate. The test conditions involved low speed crossflow velocity ($U_\infty \leq$ 100 m/sec), ambient freestream temperatures, and coolant temperatures approximately 20 degrees below ambient. Only single hole injection was investigated and the coolant hole was inclined 30 degrees in the direction of the crossflow ($\alpha_0 = 30°$). Knowing the distribution of wall temperature and the temperatures of the coolant air and the freestream, the effectiveness distribution, or footprint, was readily ascertained.

Recently a three-dimensional finite difference procedure (ref. 7) has been applied in reference 8 to the problem of predicting the flow and thermal fields arising from the injection of fluid in discrete jets through a wall into a crossflow. An example was presented to simulate a gas turbine blade cooled with a single row of holes aligned at 30 degrees to the blade surface. Such an analysis is very complicated, time consuming on the computer, requires complex boundary conditions, and does not lend itself to easy parametric variations that reflect changes in the mixing process between the coolant and freestream. One of the principal objectives of the current research is to evaluate the influence of mixing on the effectiveness. There appears to be a need for an analytical model that is amenable to parametric, or modeling, changes.

Reported herein is a two-dimensional integral method which will predict the local centerline adiabatic wall temperature and the coolant coverage area within a short dimensionless distance downstream of a 30 degree inclined coolant injection hole. Assumptions were made about the coolant layer cross-section shape and the entrainment mechanism involved in the mixing of the freestream with the coolant. Integral conservation equations governing the coolant mixing layer over the surface were formulated and solved numerically. The results of this analysis are compared to the low speed film cooling experimental results in reference 6.

ANALYSIS

The problem considered in the present study is depicted in Fig. 1. The geometry is a flat plate, with a hole of diameter D_0 whose axis makes an angle α_0 with the surface. Air coolant was injected through this hole into an external crossflow, U_∞. The coolant mixing layer changes its direction rapidly and turns towards the plate. The flow separates immediately after the injection hole. A boundary layer flow develops along the plate surface after the coolant layer reattaches to the surface.

In this analysis, the entire mixing layer is first solved with inviscid flow theory. A boundary layer effect is then included in the reattached mixing layer.

I. Inviscid Analysis

The flow field is dominated by the mixing process and the pressure gradient caused by the rapid changing in direction in the initial stage. The boundary layer flow along the wall surface is neglected and the viscous effect (τ_w) to the momentum conservation equation is not included.

A. Assumptions

(1) The flow is steady and the wall surface is adiabatic.

(2) The velocity is uniform within the cross section normal to the axis of the mixing layer.

(3) The coolant flow cross sectional area changes from a circle at the coolant exit to an ellipse at location bb (Fig. 1) and the ratio of minor axis to major axis varies linearly from 1 to 0.25 as a function of Z/D_0. Similar elliptical cross sections with $d/D = 0.25$ exist after location bb.

(4) With an adiabatic wall and low speed flow ($M < 0.3$), the local adiabatic wall temperature equals the local total temperature of the mixing layer, $T_{aw} = T$.

B. Governing Equations

The theoretical analysis of a jet injected into a crossflow (ref. 9) is utilized. The energy conservation equation is added to solve the local total temperature.

(1) Streamwise Momentum Equation

$$A \frac{dp}{dZ} + \frac{d}{dZ}\left(\int_A \rho U^2 \, dA \right) = m U_\infty \cos \theta$$

With the aid of Euler's equation of the external flow,

$$\frac{dp}{dZ} = \rho_\infty U_\infty^2 \sin \theta \cos \theta \frac{d\theta}{dZ}$$

The streamwise momentum equation becomes

$$\frac{A}{2} \rho_\infty U_\infty^2 \sin 2\theta \frac{d\theta}{dZ} + AU^2 \frac{d\rho}{dZ}$$

$$+ 2\rho UA \frac{dU}{dZ} + \rho U^2 \frac{dA}{dZ} = mU_\infty \cos \theta \qquad (1)$$

(2) Momentum Equation Normal to the Centerline

The surface forces and centrifugal body forces are equated to the momentum flux due to entrainment. The emerging jet is treated as if it were a solid body in computing its contribution to the drag. A drag coefficient C_D is utilized for this purpose and the normal force is expressed as $[C_D (\rho_\infty U_\infty^2/2) \sin^2\theta] D \, dZ$

$$C_D \frac{\rho_\infty U_\infty^2}{2} \sin^2\theta \, D + A\rho U^2 \frac{d\theta}{dZ} = -mU_\infty \sin \theta \qquad (2)$$

(3) Energy Conservation Equation

With the adiabatic wall assumption, conservation of the total enthalpy in the coolant mixing layer results in the following energy balance equation:

$$\frac{d}{dZ}\left(\int_A \rho U C_p T \, dA \right) = m C_p T_{0\infty}$$

For constant C_p, the above equation becomes

$$\rho UT \frac{dA}{dZ} + \rho UA \frac{dT}{dZ} + TA\rho \frac{dU}{dZ} + TAU \frac{d\rho}{dZ} = mT_{0\infty} \qquad (3)$$

(4) Mass Conservation Equation

The continuity equation, with entrainment effect, can be written as

$$\rho U \frac{dA}{dZ} + \rho A \frac{dU}{dZ} + UA \frac{d\rho}{dZ} = m \qquad (4)$$

(5) Equation of State

Assuming the equation of state of an ideal gas is valid in the coolant mixing layer, with the aid of Euler's equation, the equation of state can be written as

$$\frac{1}{2} \rho_\infty U_\infty^2 \sin 2\theta \frac{d\theta}{dZ} + \frac{R\rho U}{C_p} \frac{dU}{dZ} - R\left(T - \frac{U^2}{2C_p} \right) \frac{d\rho}{dZ} - R\rho \frac{dT}{dZ} = 0$$

$$(5)$$

where R is the ideal gas constant.

(6) Entrainment Mass Flow Rate, m

To solve U, ρ, T, A, and θ from equations (1) to (5), the entrainment mass flow rate must be estimated. The following correlation similar to the equation used in reference 10 is employed:

$$m = \rho_\infty E_1 U_\infty D \sin \theta$$

$$+ (\rho_\infty E_2 |U - U_\infty \cos \theta| C)/2/(1 + E_3 U_\infty \sin \theta/U) \qquad (6)$$

where E_1, E_2, and E_3 are empirical constants. The effect of the approaching freestream particles to jet entrainment is modeled in the

first term of the right side of equation (6) and the extrainment due to the freestream moving along the edge of the coolant layer is accounted for by the second term. In surface film cooling, the coolant layer attaches to the wall surface and a factor of 2 was inserted in equation (6) to consider the effective unit surface area for entrainment evaluation in the present inviscid analysis.

C. Cross Sectional Area of the Coolant Mixing Layer

Employing assumption (3), geometric relations for the mixing layer cross sectional area are derived.
From aa to bb in Fig. 1,

$$d/D = 1 - 0.433 (Z/D_0)$$

$$C = \pi D \left[\frac{1 + (1 - 0.433 \, Z/D_0)^2}{2} \right]^{1/2} \qquad (7)$$

After location bb,

$$d/D = 0.25, \quad C = 2.24D, \quad A = \pi D^2/16 \qquad (8)$$

II. Boundary Layer Effect

The effect of boundary layer development along the adiabatic wall surface after the reattachment of the coolant mixing layer is considered. A two-dimensional boundary layer is assumed.

A. Assumptions

(1) The pressure distribution is imposed by the main cross flow and the streamwise pressure gradient is zero due to constant U_∞.
(2) The wall beneath the boundary layer is adiabatic.
(3) Both laminar and turbulent boundary layers are considered. Expressions for flat plate boundary layer parameters are valid.
(4) The local total temperature is constant across the boundary layer and the local static temperature equals the local total temperature within the low speed mixing layer.

B. Governing Equations

Principles for the development of the governing equations are similar to section I-B. This technique has also been used in reference 5 for tangential slot injection.

(1) Continuity Equation

$$\frac{d}{dZ}\left[\rho U(H - \delta) \right] + \frac{d}{dZ}\left(\int_0^\delta \rho U_b \, dY \right) = m \qquad (9)$$

(2) Z-momentum Equation

$$\frac{d}{dZ}\left[\rho U^2(H - \delta) \right] + \frac{d}{dZ}\left(\int_0^\delta \rho U_b^2 \, dY \right) = \tau_\infty + mU_\infty \qquad (10)$$

(3) Energy Equation

$$\frac{d}{dZ}\left[\rho U(H - \delta)T \right] + \frac{d}{dZ}\left(\int_0^\delta \rho U_b T \, dY \right) = mT_{0\infty} \qquad (11)$$

3

(4) Equation of State

$$\rho \frac{dT}{dZ} + T \frac{d\rho}{dZ} = 0 \tag{12}$$

(5) Entrainment Mass Flow Rate

For two-dimensional flow and $\theta = 0$, equation (6) becomes

$$\dot{m} = \rho_\infty E_2 |U - U_\infty| \tag{13}$$

(6) Boundary Layer Parameters (ref. 11)

For laminar boundary layer

$$\delta = 5 \left(\frac{\mu X}{\rho U}\right)^{1/2}$$

$$\tau_w = 0.332 \ \rho U^2 \left(\frac{\rho U X}{\mu}\right)^{-1/2} \tag{14}$$

$$\frac{U_b}{U} = 2 \left(\frac{y}{\delta}\right) - 2 \left(\frac{y}{\delta}\right)^3 + \left(\frac{y}{\delta}\right)^4$$

For turbulent boundary layer

$$\delta = 0.37 \ X \left(\frac{U X \rho}{\mu}\right)^{-0.2}$$

$$\tau_w = 0.0225 \ \rho U^2 \left(\frac{\rho U \delta}{\mu}\right)^{-0.25} \tag{15}$$

$$\frac{U_b}{U} = \left(\frac{y}{\delta}\right)^{1/7}$$

III. Method of Solutions to the Governing Equations

Equations (1) to (5) were solved for the first derivatives of the flow variables as functions of the variables, i.e.,

$$\frac{df_i}{dZ} = F_i(\rho, U, T, A, \theta) \tag{16}$$

where $f_i = \rho, U, T, A,$ or θ.

Including the boundary layer flow effect, equations similar to equation (16) can be derived by substituting the assumption, equations (14) and (15), into equations (9) to (11), and resulted as

$$\frac{dg_i}{dZ} = G_i(\rho, U, H) \tag{17}$$

where $g_i = \rho, U,$ or H.

These two sets of equations were solved numerically as initial value problems, using the fourth order Runge-Kutta method, to determine the local values of ρ, U, T, θ, A (or H). Coolant existing conditions were the initial conditions for equation (16). The inviscid flow solution from equation (16) at the location where $\theta \approx 0$ were used as the initial conditions in solving equation (17). The local total temperature, with the boundary layer effect, was obtained from equation (12) after the local density was computed from equation (17). With the assumption that the local total temperature equals the local adiabatic wall temperature in

a low speed coolant mixing layer, the local effectiveness, $\eta = (T_{0\infty} - T_{aw})/(T_{0\infty} - T_{0c}) = (T_{0\infty} - T)/(T_{0\infty} - T_{0c})$ could be computed from these numerical results.

RESULTS AND DISCUSSION

I. Inviscid Analysis

Different values of the empirical constants, C_D, E_1, E_2, and E_3 have been used in equations (16) to find the best agreement in local adiabatic wall temperatures from the numerical solution and the experiment (ref. 6). The process failed to yield a unique value of E_1 which will give satisfactory agreement for different injection rates. Film cooling effectiveness, based on the computed adiabatic wall temperature with $C_D = 2$, $E_2 = 0.08$, $E_3 = 30$, and $E_1 = 0.2$ and 0.3 respectively for $\lambda = 0.37$ and 0.54 are compared with experimental data in Figs. 2 and 3. The present inviscid analysis predicts the centerline distribution of the film cooling effectiveness over most of the centerline. However, there is large discrepancy for $Z/D_0 \leq 1$. The effective coverage area, computed from equations (7) and (8) are also shown with experimental data in Figs. 4 and 5. The experimental data are based on the isotherm footprints for $\eta = 0.1$. A smaller effective area was computed than was observed experimentally.

The entrainment mass flow rates for $\lambda = 0.37$ and 0.54 with prescribed empirical constants are compared in Fig. 6. The effects of constant E_2 and the flow direction are significant for $Z_0/D_0 \leq 3$. After $Z_0/D_0 = 3$, a smaller entrainment rate was computed for $\lambda = 0.54$ than $\lambda = 0.37$ due to the velocity difference within the coolant layer.

To investigate the present geometry assumptions, the inviscid flow direction, major axis of the elliptical cross section, and the differences between the normal distance from the center of the analytical mixing layer to the wall and half of the minor axis are plotted for $\lambda = 0.37$ in Fig. 7. The flow angle, θ, within the coolant layer decreases rapidly from location aa to location bb. After location bb, a small flow angle, θ, was computed. Very small difference between e and $d/2$ was found. These computational results show that the coolant layer does not separate from the wall surface with $\alpha_0 = 30$ degrees and $\lambda = 0.37$. This is consistent with the flow visualization results in reference 12.

II. Boundary Layer Effect

Results of the analysis with the boundary layer effect are also given in Figs. 2 to 5. The initial conditions for the numerical solution were obtained from the inviscid solution corresponding to the location with $\theta = 0$. These locations corresponded to $Z/D_0 = 0.8$ for $\lambda = 0.37$ and $Z/D_0 = 1.1$ for $\lambda = 0.54$. When compared to the inviscid flow analysis, lower adiabatic wall temperatures were predicted. A laminar boundary layer assumption predicts higher effectiveness than the turbulent boundary layer case. This is consistent with less mixing in a laminar coolant layer. The local Reynolds number, $\rho U X/\mu$, within the coolant mixing layer was computed and found to be of the order of 10^5 after $Z/D_0 \approx 2$. Thus, a turbulent boundary layer assumption predicts the existing experimental results better than the laminar

4

assumption. For the present studies, expressions
for the wholly developed boundary layer velocity
profile, shear stress, and boundary layer thickness
were used. To model the boundary layer effect
downstream of a discrete hole injection, detail
profiles of velocity, coolant concentration, and
turbulence are required. Moreover, coolant injec-
tion will significantly reduce the local skin fric-
tion in a region close to the injection. There-
fore, the assumptions made in Section II-B may have
contributed to the difference between the analysis
and experiment in Figs. 2 and 3. Assuming the
coolant mixing layer cross section is an ellipse
with $H/D = 0.25$ and using the H values obtained
from the turbulent boundary layer assumption, the
coolant coverage area was also computed and shown
in Figs. 4 and 5. It differs slightly from the
results of the inviscid analysis.

III. Comparison with Existing Analysis

Recently, analyses have been performed for
single and multiple hole surface film cooling by
numerical solution of the three-dimensional flow
field (refs. 7 and 8). The analyses are effective
in computing the average film cooling effectiveness
far downstream of the injection hole but are time
consuming in numerical computation. Equivalent
technique based on tangential slot injection has
also been proposed to compute the initial condi-
tions for a boundary layer flow analysis due to
inclined hole injection (ref. 3). The analysis
presented herein is simple in computation and
effective in predicting the centerline local adia-
batic wall temperature and the effective coolant
coverage area near the injection hole. However, a
general correlation for the entrainment mass flow
rate, which would be valid for different injection
rates, was not found in this study. The assump-
tions about the coolant mixing layer cross section
also need further confirmation. Due to the assump-
tion made in local total temperature and adiabatic
wall temperature, the present method is also
limited to a low speed coolant mixing layer.

SUMMARY

Assuming the local adiabatic wall temperature
equals the local total temperature, an analysis has
been developed to compute the centerline film cool-
ing effectiveness and coolant coverage area beneath
the coolant mixing layer downstream of a single
film coolant injection hole inclined at 30 degrees
to the crossflow. Integral conservation equations
are formulated and solved numerically to determine
the local adiabatic wall temperature and coolant
spreading. Inviscid analysis, assuming elliptical
cross section in the mixing layer, predicts the
film cooling effectiveness within a small distance
downstream of the injection hole. Lower adiabatic
wall temperature (higher effectiveness) is found
from a two dimensional analysis with a boundary
layer effect. Smaller spanwise coolant spreading
than the direct measurement from the experiment is
computed from the present analytical methods.
The present analysis is simple and its numer-
ical results compared favorably with infrared mapp-
ing of the adiabatic wall temperature from an
existing film cooling experiment. However, this
analysis is subject to further confirmation per-
taining to the assumptions about the mixing layer
geometry and entrainment rate.

REFERENCES

1 Hatch, J. E., and Papell, S. S., "Use of a
Theoretical Flow Model to Correlate Data for Film
Cooling or Heating on Adiabatic Wall by Tangential
Injection of Gases of Different Fluid Properties,"
NASA TN D-130, 1959.

2 Stollery, J. L. and El-Ehwany, A. A. M.,
"A Note on the Use of a Boundary Layer Model for
Correlating Film Cooling Data, International
Journal of Heat and Mass Transfer, Vol. 8, Jan.
1965, pp. 55-65.

3 Louis, J. F., "Heat Transfer in Turbines,"
Technical Report AFAPL-TR-75-107, Sept. 1975.
(AD-A021256.)

4 Jabbari, M. Y., and Goldstein, R. J.,
"Effect of Mainstream Acceleration on Adiabatic
Wall Temperature and Heat Transfer Downstream of
Gas Injection," International Heat Transfer
Conference, 6th, Toronto, CANADA, August 1978,
General Papers, Vol. 5, Hemisphere Publishing
Corp., Washington, D.C., pp. 249-254.

5 Goldstein, R. J., Eriksen, V. L., and
Ramsey, J. W., "Flow and Temperature Fields Follow-
ing Injection of a Jet Normal to a Cross Stream,"
International Heat Transfer Conference, 6th,
Toronto, CANADA, August 1978, General Papers,
Vol. 5, Hemisphere Publishing Corp., Washington,
D.C., pp. 255-260.

6 Papell, S. S., Graham, R. W., and
Cageao, R. P., "Influence of Coolant Tube Curvature
on Film Cooling Effectiveness as Detected by
Infrared Imagery," NASA TP-1546, November 1979.

7 Patankar, S. V., and Spalding, D. B.,
"A Calculation Procedure for Heat, Mass and Momen-
tum Transfer in Three-Dimensional Parabolic Flow,"
International Journal of Heat and Mass Transfer,
Vol. 15, Oct. 1972, pp. 1787-1806.

8 Bergeles, G., Gosman, A. D., and
Launder, B. E., "The Prediction of Three Dimen-
sional Discrete-Hole Cooling Processes, Part 1:
Laminar Flow" Journal of Heat Transfer, Vol. 98,
No. 3, Aug. 1976, pp. 379-386.

9 Adler, D., and Baron, A., "Prediction of a
Three-Dimensional Circular Turbulent Jet in Cross-
flow," AIAA Journal, Vol. 17, No. 2, Feb. 1979,
pp. 168-174.

10 Wooler, P. T., Burghart, G. H., and
Gallagher, J. T., "Pressure Distribution on a
Rectangular Wing with a Jet Exhausting Normally
into an Airstream," J. Aircraft, Vol. 4, No. 6,
Nov.-Dec. 1967, pp. 537-543.

11 Schlichting, H., Boundary-Layer Theory,
7th. ed., McGraw-Hill, New York, 1979.

12 Colladay, R. S., Russell, L. M., and
Lane, J. M., "Streakline Flow Visualization of Dis-
crete Hole Film Cooling with Holes Inclined 30° to
Surface," NASA TN D-8175, 1976.

D_o

aa CROSS SECTION

D

d

SIMILAR ELLIPTIC CROSS SECTION AFTER bb

INJECTION HOLE

D

ρ_∞, U_∞

COOLANT MIXING LAYER

b

a m

Z m

u

θ

Z_o

SEPARATION e BOUNDARY LAYER

ADIABATIC WALL

c_o

b

ρ_j, U_j

a

Figure 1. - Schematic of problem considered.

O EXPERIMENT (REF. 6)
INVISCID ANALYSIS
TURBULENT BOUNDARY LAYER
LAMINAR BOUNDARY LAYER

FILM COOLING EFFECTIVENESS, $\eta = \dfrac{T_{\infty} - T_{aw}}{T_{\infty} - T_{oc}}$

1.0

.8

.6

.4

0 1 2 3 4 5 6 7 8

DISTANCE FROM INJECTION HOLE, Z/D_o

Figure 2. - Centerline film cooling effectiveness, $\lambda = 0.37$.
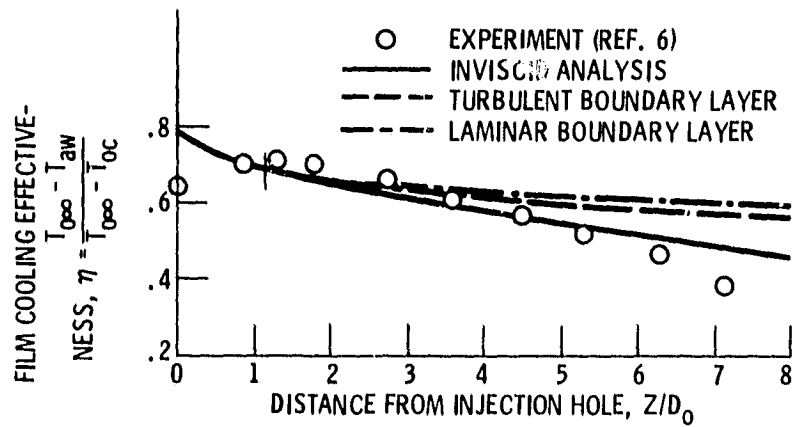
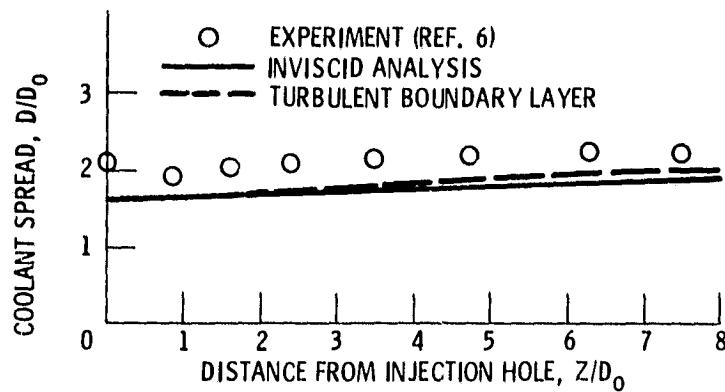Figure 3. - Centerline film cooling effectiveness, $\lambda = 0.54$.

Figure 4. - The spanwise spread of the coolant, $\lambda = 0.37$.

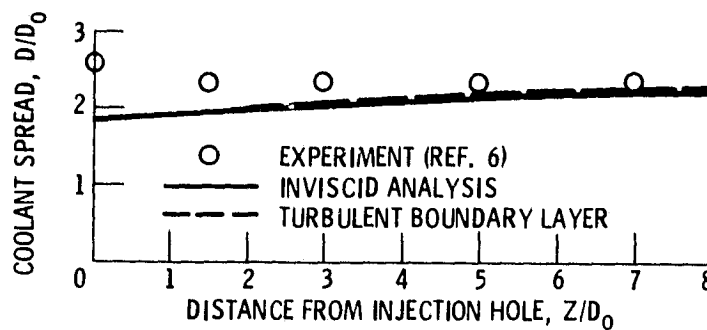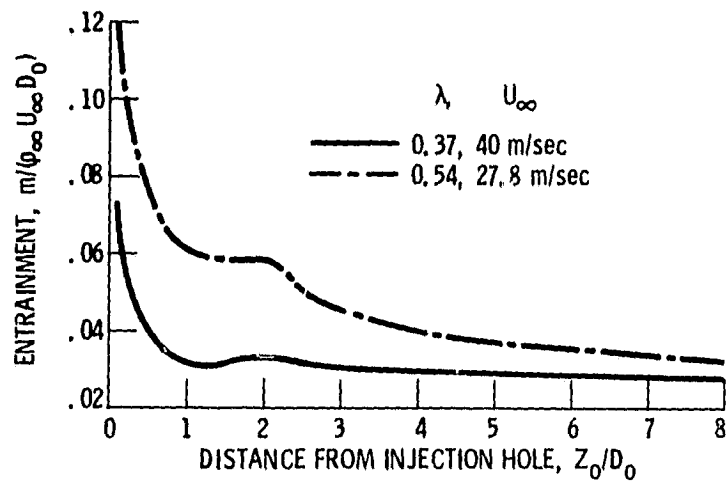Figure 5. - The spanwise spread of the coolant, $\lambda = 0.54$.

λ, U∞

0.37, 40 m/sec

0.54, 27.8 m/sec

ENTRAINMENT, m/(φ∞ U∞ D₀)

DISTANCE FROM INJECTION HOLE, Z_0/D_0

Figure 6. - Entrainment mass flow rates, inviscid flow analysis.

$α_0 = 30°$, $λ = 0.37$

θ, FLOW DIRECTION

D/D_0, DIMENSIONLESS MAJOR AXIS

$(e - 0.5 \, d)/D_0$, SEPARATION DISTANCE

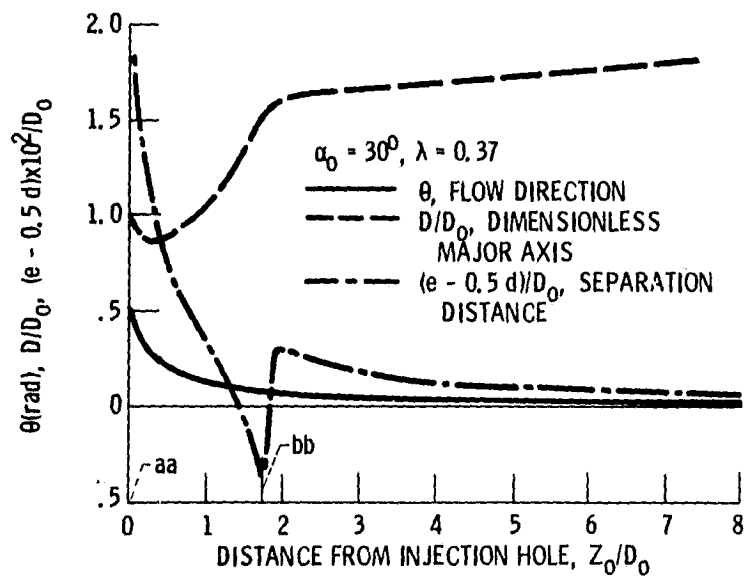θ(rad), D/D_0, $(e - 0.5 \, d) \times 10^2/D_0$

aa

bb

DISTANCE FROM INJECTION HOLE, Z_0/D_0

Figure 7. - Geometry of the inviscid mixing layer.